A method to determine γ branching ratios using charged particle detectors for states in ^{18}O

Pirrie, S.; Kokalova, Tz; Wheldon, C.; Bailey, S.; Bishop, J.; Curtis, N.; Smith, R.; Torresi, D.; Turner, A.; Hertenberger, R.; Wirth, H. F.; Faestermann, Th; Mengoni, D.; Dell'Aquila, D.

DOI:
10.1063/1.5078856

A method to determine γ branching ratios using charged particle detectors for states in ^{18}O

S. Pirrie[1,a),*], Tz. Kokalova[1], C. Wheldon[1], S. Bailey[1], J. Bishop[1], N. Curtis[1], R. Smith[1], D. Torresi[1], A. Turner[1], R. Hertenberger[2], H.-F. Wirth[2], Th. Faestermann[3], D. Mengoni[4] and D. Dell'Aquila[5]

[1]*School of Physics and Astronomy, University of Birmingham, Edgbaston Park Rd, Birmingham, UK, B15 2TT*
[2]*Fakultät für Physik, Ludwig-Maximilians-Universität München, D-85748 Garching, Germany*
[3]*Physik Department, Technische Universität München, D-85748 Garching, Germany*
[4]*Università degli Studi di Padova, Via 8 Febbraio 1848, 2, 35122 Padova PD, Italy*
[5]*Università degli Studi di Napoli Fedorico II, Corso Umberto I, 40, 80138 Napoli NA, Italy*

[a)]Corresponding author: S.Pirrie@PGR.bham.ac.uk

Abstract. A series of proposed bands in ^{18}O with potential nuclear molecular structures, such as ^{14}C $\bigotimes$ α or ^{12}C $\bigotimes$ $2n$ $\bigotimes$ α, are being investigated. This was done through the use of the Q3D magnetic spectrograph at the Maier-Leibnitz Laboratory in Munich in conjunction with an array of double-sided silicon strip detectors (DSSDs). These detectors allowed for high resolution reconstruction of detected particles, enabling measurement of the branching ratios of the states that make up these bands. Here, a method is discussed for extracting the branching ratios of both material particles as well as γ-particles using the DSSD array to detect only charged decay fragments.

INTRODUCTION

Nuclear clustering is a well-established phenomenon observed in several nuclei, but the most common of these are light, even $N = Z$ nuclei [1] [2]. Clustering, however, is proposed to occur in many nuclei that are not purely alpha-conjugate. The addition of a pair of neutrons to the system can decrease the required threshold for an alpha particle to form in the nucleus, as in the case with ^{16}O (7.16 MeV threshold for a ^{12}C $\bigotimes$ α structure) going to ^{18}O (6.23 MeV threshold for a ^{14}C $\bigotimes$ α structure).

An excellent contender for the observation of cluster structure is ^{18}O, particularly a core + alpha description due to the properties of both the α and ^{14}C nucleus. Like ^{16}O (a cluster core observed most clearly in the core + alpha description of ^{20}Ne [3][4]), ^{14}C has a closed p-shell and its first excited state lies at around 6 MeV, lending more credence to the notion of a ^{14}C $\bigotimes$ α configuration in ^{18}O.

An experiment performed at the Maier-Leibnitz Laboratory (MLL) of the Technical University and Ludwig-Maximillan University in Munich by W. von Oertzen *et al.* found 30 previously unobserved states in ^{18}O [5]. Using these and previously measured states, rotational bands with different nucleon configurations were proposed. The states that make up these proposed rotational bands are shown in **TABLE 1**. As these proposed bands, each with an associated positive and negative parity due to signature splitting, have a cluster structure, with the $K^{\pi} = 0_2^{+/-}$ proposed to have a ^{14}C $\bigotimes$ α structure and the $k^{\pi} = 0_4^{+/-}$ proposed to have a ^{14}C $\bigotimes$ α structure, the associated partial α decay widths of the composite states can be used to confirm or refute the existence of each band as levels built upon the same configuration should have similar decay properties.

*Work supported by STFC (UK)

TABLE 1: The preliminary measured excitation energies and FWHMs of states in the proposed rotational bands compared to the literature values for the excitation energies and widths from Ref. [5]. Spins and parities that were assigned based on fitting the rotational properties are shown in brackets, and states with a small cross-section (<2 μb/sr) with an asterisk (*). The resolution of the focal plane varied across its length and was determined for the ground state (measured FWHM of 86(5) keV) and the 1^{st} excited state (measured FWHM of 76(3) keV), measured at separate ends of the focal plane detector. Unmeasured states lay outside of the excitation regions investigated.

$K^\pi = 0_2^+$				
E_x (MeV)	FWHM (keV)	$E_{x,Lit}$ (MeV)	Γ_{Lit} (keV)	J^π_{Lit}
unmeasured		3.558(4)	-	0^+
unmeasured		5.254(5)	-	2^+
7.114(1)	80 (2)	7.115(4)	-	4^+
11.716(4)	95 (11)	11.702(6)	27	6^+
unmeasured		18.058(8)	83	8^{+}*

$K^\pi = 0_2^-$				
E_x (MeV)	FWHM (keV)	$E_{x,Lit}$ (MeV)	Γ_{Lit} (keV)	J^π_{Lit}
8.037(1)*	93(19)	8.035(5)	<10	1^-
9.737(4)	118(7)	9.715(5)	15(4)	(3^-)
13.617(3)	-	13.624(6)	22(7)	(5^-)
unmeasured		18.630(10)	100(20)	(7^-)

$K^\pi = 0_4^+$				
E_x (MeV)	FWHM (keV)	$E_{x,Lit}$ (MeV)	Γ_{Lit} (keV)	J^π_{Lit}
7.798(1)*	-	7.796(5)	<10	0^+
8.217(1)	66(3)	8.216(4)	<10	2^+
10.297(5)	84(5)	10.293(4)	23(8)	4^+
12.559(1)	114(7)	12.557(6)	22(8)	6^+
unmeasured		15.810(10)	20(8)	(8^+)
unmeasured		20.385(15)	155(25)	(10^+)

$K^\pi = 0_4^-$				
E_x (MeV)	FWHM (keV)	$E_{x,Lit}$ (MeV)	Γ_{Lit} (keV)	J^π_{Lit}
10.595(4)	105(7)	10.59(1)	70(16)	(1^-)
10.937(4)	99(6)	10.92(1)	30(9)	(3^-)
13.827(3)	80(4)	13.82(2)	27(8)	(5^-)
unmeasured		16.99(1)	50(12)	(7^-)
unmeasured		20.28(3)	120(21)	(9^-)

EXPERIMENTAL METHOD

A subsequent experiment was performed, also at MLL Munich, to determine the branching ratios of the high-energy excited states in ^{18}O and hence extract their partial α decay widths. The reaction chosen to populate states in ^{18}O was ^{12}C(^{7}Li,p)^{18}O* (Q_0 = +8.401 MeV) as this reaction, used by von Oertzen *et al.*, was known to be well-populated. The 15 MV tandem Van de Graaff accelerator at MLL was used to produce a 44 MeV ^{7}Li beam. The Q3D spectrograph was set at an angle of −39° in the horizontal beam plane, with an angular acceptance of ±3° in x (horizontal) and ±2° in y (vertical). The Birmingham array of 50 mm by 50 mm, 500 μm thick double-sided silicon strip detectors (DSSDs) was used in conjunction with the Q3D spectrograph in order to extract both energy and momentum information, allowing for high-resolution reconstruction. The experimental set-up and DSSD array are depicted in **FIGURE 1**.

The Q3D spectrograph was configured to allow for the detection of the resulting protons from the reaction. The Q3D consists of a scintillator for measuring the energy of an incident particle, two upstream horizontal wires in a gas volume for measuring the energy loss and a 255 strip cathode foil for measuring the position of incident particles [6]. Using the information from the scintillator and the horizontal wires, particle identification was achieved and hence proton-only events were selected. The energy of the proton is obtained from the detected position at the focal plane [7] and enables an excitation spectrum for ^{18}O to be produced. An example of this is shown later in **FIGURE 5**. It should be noted that the position of the proton at the focal plane was independent of the angle at which it entered the Q3D. The corresponding ^{18}O or its decay products would then, in the majority of cases, be detected by the DSSD array, which had a total angular coverage of 14° to 92° in-plane, and −36° to 40° out-of-plane. When an event was registered in the Q3D, all events in the ADC channels of the DSSDs were read out, allowing for events with Q3D and DSSD coincidences as well as Q3D-only events.

RESULTS

As the particles incident on the DSSDs were not directly identified, a technique to identify a detected particle-species based on its energy and momentum was adopted. In the break-up of ^{18}O* into particles A and B, using events with a single hit in the DSSD array (for example, a detection of A), the momentum of the undetected B can be reconstructed:

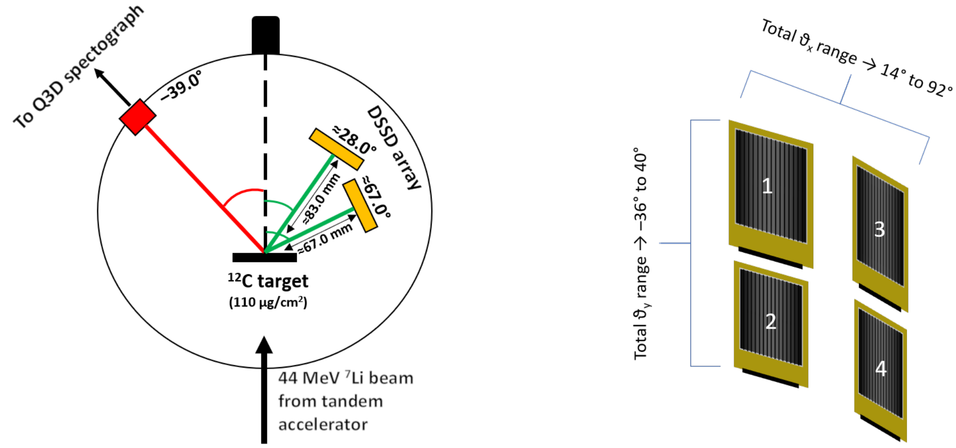

(a) (b)

FIGURE 1: Diagrams illustrating the experimental set-up used at MLL. The plan view in the chamber is shown in (a), while the double-sided silicon strip detector (DSSD) array is shown in more detail in (b). The in-plane center angle of detectors 1 and 2 was +28±1° and for detectors 3 and 4 was +67±1°. The out-of-plane center angles of detectors 1-4 were +21±1°, −15±1°, +25±1° and −18±1° respectively.

$$\vec{p_B} = \vec{p_{beam}} - \vec{p_{Q3D}} - \vec{p_A}, \tag{1}$$

where $\vec{p_A}$ is the momentum of the particle detected in the DSSD array, $\vec{p_{beam}}$ is the momentum of the beam particle and $\vec{p_{Q3D}}$ is the momentum of the proton detected at the Q3D focal plane [8]. The momentum in each Cartesian direction can be calculated using the angles of detection of any detected particles in conjunction with their energies and masses. Using particle A as an example:

$$\begin{aligned} p_A &= \sqrt{2E_A m_A}, \\ p_{A_x} &= p_A \sin\theta_x \cos\theta_y, \\ p_{A_y} &= p_A \sin\theta_y \quad \text{and} \\ p_{A_z} &= p_A \cos\theta_x \cos\theta_y, \end{aligned} \tag{2}$$

with θ_x and θ_y being the angles of detection in-plane and out-of-plane respectively. In order to calculate the total momentum of the detected particle, the mass (m_A) must be assumed.

Using this information, the total momentum of the missing particle can then be substituted into the Q value expression for the ^{12}C(^{7}Li,p)A+B reaction,

$$Q = E_A + E_{Q3D} + \frac{p_B^2}{2m_B} - E_{beam}, \tag{3}$$

where the energy of particle B has been related to its momentum by $E_B = \frac{p_B^2}{2m_B}$. Rearranging this to be in the form $y = mx + c$ gives the following expression,

$$E_{beam} - E_A - E_{Q3D} = \frac{p_B^2}{2m_B} - Q, \tag{4}$$

which allows the calculated value of $\frac{p_B^2}{2}$ to be plotted against the measured value of $E_{beam} - E_A - E_{Q3D}$, generating a locus with a gradient of $1/m_B$ and a y-intercept of $-Q$ if the correct assumption has been made regarding the mass of the particle in Equation 2. If a detected particle does not have the same mass as the one assumed, the associated locus will not lie on the line described by this gradient and y-intercept. Such a diagram is known as a Catania plot, and **FIGURE 2** shows a labeled example.

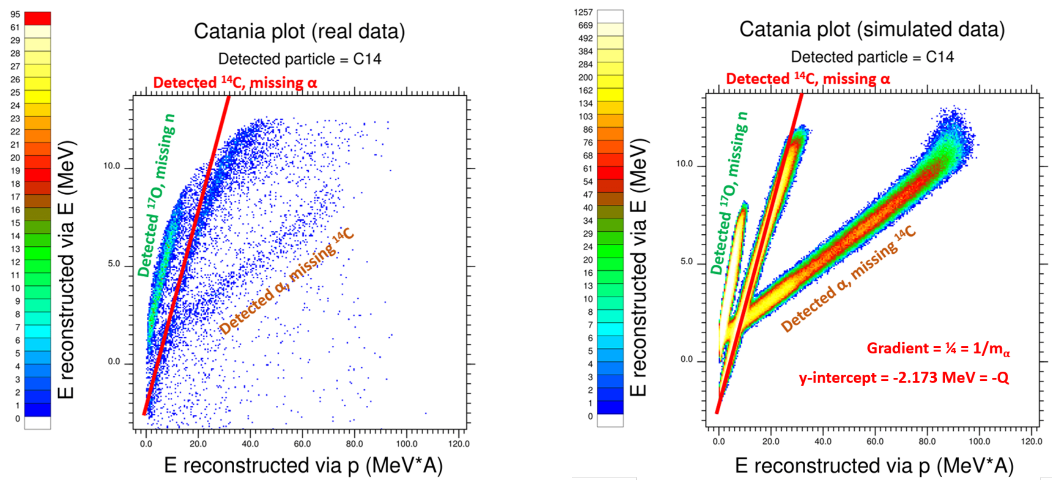

(a) (b)

FIGURE 2: A comparison of experimental (a) and simulated (b) data plotted on a Catania plot. The simulated data were produced using Resolution8.1 [9][10], an in-house Monte Carlo simulation package, and contain 2 types of break-up: ^{12}C(^{7}Li,p)α+^{14}C (Q = +2.173 MeV) and ^{12}C(^{7}Li,p)n+^{17}O (Q = +0.355 MeV). The momenta for all particles detected in the DSSD were calculated assuming they were ^{14}C, allowing correct events to lie on the locus defined by the red line with y-intercept = $-Q$ = -2.173 MeV and gradient = $\frac{1}{m_\alpha}$. Incorrect assumption of the particle mass cause the other visible loci to arise, but these are still distinct from one another and allow for particle identification when compared with simulation.

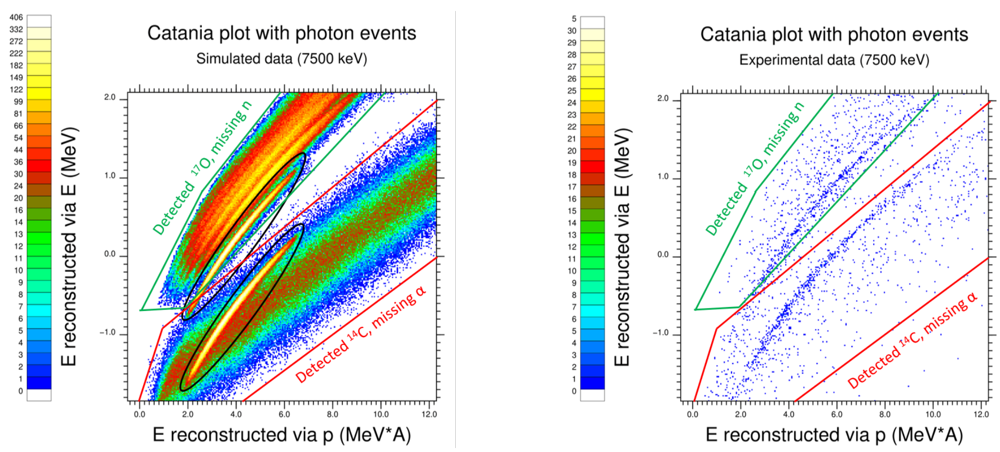

(a) (b)

FIGURE 3: A comparison of simulated data (a) and experimental data (b), scaled to show low reconstructed energy events, which demonstrates the agreement between the simulation of the 7.115 MeV 4^+ state in ^{18}O decaying to the 6.404 MeV 3^- state and the 7.969 MeV state $3^+/4^-$ photon decaying to the 6.880 MeV 0^- state (both highlighted in black ellipses). The simulation includes the decay modes mentioned in **FIGURE 2**, which are labelled in both (a) and (b) and can be seen to be in good agreement.

Photon Events

States that have a significant γ decay branch, such as unnatural parity states below the n decay threshold (8.045 MeV), will also be present on a Catania plot, but due to the small amount of momentum taken by the photon the loci formed by γ decay events will contaminate other loci from massive particle decay with a large variability depending on the γ-ray energy of the associated decay. As one of the excitation regimes investigated in this analysis was centered around

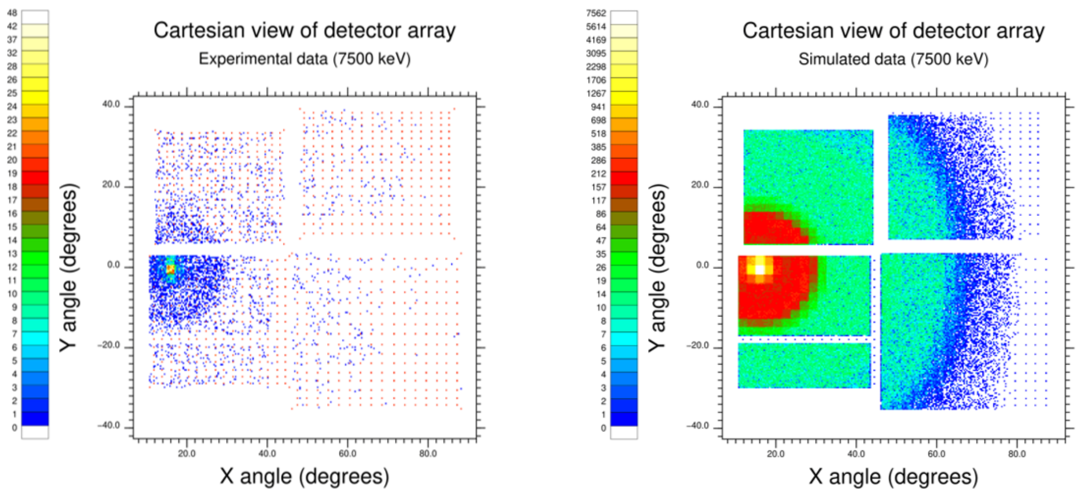

(a) (b)

FIGURE 4: Two-dimensional plots showing the number of events hitting each pixel of the detector, with events smeared randomly across the area of the pixel (9 mm^2). Experimental data are shown in (a) while simulated data are shown in (b). The region in the center of the Gaussian profiles with the largest number of counts is largely formed by the focused nature of the ^{18}O distribution, which is confirmed using the simulation to identify features. The pixel centers of the detectors of the detectors are shown by the grid of points for both experimental and simulated data.

7500 keV, several states might be expected to decay via photon emission. An example of this contamination can be seen in **FIGURE 3**, along with simulation comparisons using two states (7.115 MeV and 7.969 MeV) which match well to the observed features in the data.

As the γ events prevent gating on the loci formed due to massive particles, they must be removed in order to establish branching ratios for the various decay modes. This can be achieved through plotting the in-plane and out-of-plane Cartesian angles for detections in the DSSD array on a 2D histogram and observing the Gaussian distributions due to each particle, as shown in **FIGURE 4**. The momentum of an ^{18}O nucleus detected in the DSSD array is largely defined by the momentum of the proton detected at the focal plane (as the photon takes very little), which results in a very small Gaussian distribution for ^{18}O relative to other similar particles which share momentum with massive decay products, such as ^{17}O with the n. Thus, by putting a gate around the possible ^{18}O detection region, which was confirmed through comparison with Monte Carlo simulation, γ events were removed from the Catania plot to facilitate accurate measurement of the branching ratios for each decay mode. **FIGURE 5** shows the comparison of the total excitation spectrum to that formed when looking at Q3D events coincident with a hit in the DSSD array inside the ^{18}O gate.

The ^{18}O gate also contained events from the other decay modes which needed to be accounted for in the branching ratio determination. Considering a single excitation and a single decay mode, the fraction of events outside of the ^{18}O gate was calculated from the Monte Carlo simulations using the relationship

$$f = \frac{N_{simtot} - N_{simgate}}{N_{simtot}}, \tag{5}$$

where N_{simtot} is the total number of simulated events and $N_{simgate}$ is the number of these events in ^{18}O the gate.

Using this fraction, the total number of erroneous events in the ^{18}O gate, N_{gate}, belonging to this decay mode was determined from the number of events in the γ-removed Catania plot, N_{cat}, by

$$N_{gate} = \frac{N_{cat}}{f} - N_{cat}. \tag{6}$$

Hence, N_{gate} was hence subtracted for each state in the ^{18}O-gated excitation spectrum, leaving only true γ decay events once this process was done for all decay modes. The γ decay branching ratio was then established for each state.

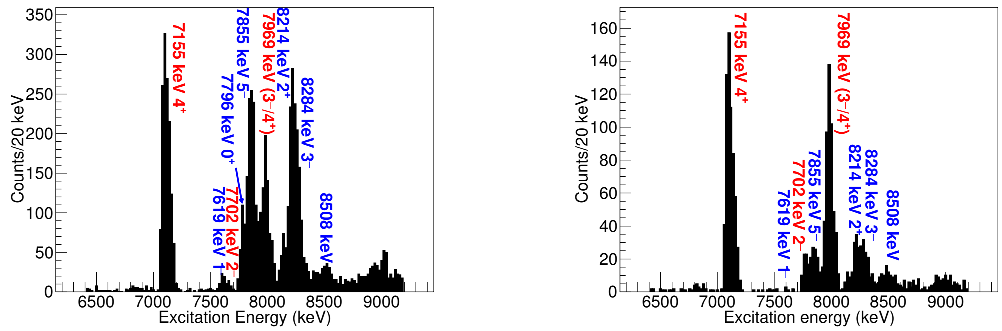

(a) (b)

FIGURE 5: A comparison of the total excitation spectrum produced centered at 7500 keV (a) with the excitation spectrum produced when gating on DSSD array hits in the ^{18}O gate (b). States that are likely to γ decay are shown in red, due to low barrier penetrability in the case of the 7.115 MeV state and the unnatural parity of the 7.770 MeV and 7.969 MeV states, which are below the n threshold of 8.045 MeV. Enhancements of these states relative to the states labelled in blue can be observed in (b).

CONCLUSION

The experimental method for measuring the branching ratios of excited states in ^{18}O has been discussed, including a technique that allows for the measurement of the γ decay branching ratio through the use of a DSSD array solely detecting charged particles. States which are expected to γ decay due to their spin-parity and excitation energy relative to decay thresholds have been investigated through use of Monte Carlo simulations and found to match observed features in experimental data Catania plots, which can then be removed and hence accurate determination of both massive particle decay and γ decay branching ratios achieved.

ACKNOWLEDGMENTS

The authors would like to thank Andy Bergmaier for his help loaning equipment during the set-up of the experiment, as well as the operators of the tandem Van de Graaff accelerator at the Maier-Leibnitz Laboratory in Munich for providing and maintaining the ^{7}Li beam. This work was funded by the UK Science and Technology Facilities Council (STFC) under Grant No. ST/L005751/1 and from the European Unions Horizon 2020 research and innovation programme under the Marie Skłodowska-Curie Grant Agreement No. 65F9744.

REFERENCES

[1] M. Freer, Rep. Prog. Phys **70**, 2149–2210 (2007).
[2] B. Fulton, Contemp. Phys **40(5)**, 299–311 (1999).
[3] W. von Oertzen *et al.*, Eur. Phys. J. A **11**, 403–411 (2001).
[4] J. Hiura *et al.*, Progr. Theor. Phys **42**, 555–580 (1969).
[5] W. von Oertzen *et al.*, Eur. Phys. J. A **43**, 17–33 (2010).
[6] H.-F. Wirth, Ph.D. thesis, Technischen Universität, München 2001.
[7] H.-F. Wirth *et al.*, Beschleuniger Laboratorium Munchen, Annual Report **(unpublished)**, p. 71 (2000).
[8] C. Wheldon *et al.*, Phys. Rev. C **83**, 2503–2504 (2011).
[9] N. Curtis *et al.*, Phys. Rev. C **51**, 1554–1557 (1995).
[10] N. Curtis *et al.*, Phys. Rev. C **53**, 1804–1810 (1996).
[11] N. Curtis *et al.*, Phys. Rev. C **66**, 024315:1–10 (2002).
[12] H. Fortune, Phys. Rev. C **18**, p. 1053 (1978).
[13] K. Artemov, Sov. J. Nucl. Phys. **37**, p. 805 (1983).
[14] G. Morgan, Nucl. Phys. A **148**, p. 480 (1970).